Photo-controllable Azobenzene Microdroplets on an Open Surface and their Application as Transporters

Journal:	*Materials Horizons*
Manuscript ID	MH-COM-10-2023-001774.R1
Article Type:	Communication
Date Submitted by the Author:	20-Nov-2023
Complete List of Authors:	Norikane, Yasuo; National Institute of Advanced Industrial Science and Technology Tsukuba Center Tsukuba Central, Ohnuma, Mio; National Institute of Advanced Industrial Science and Technology Tsukuba Center Tsukuba Central Kwaria, Dennis; University of Tsukuba, ; National Institute of Advanced Industrial Science and Technology Tsukuba Center Tsukuba Central, Kikkawa, Yoshihiro; National Institute of Advanced Industrial Science and Technology (AIST), Ohzono, Takuya; AIST, a. Electronics and Photonics Research Institute Mizokuro, Toshiko; National Institute of Advanced Industrial Science and Technology Tsukuba Center Tsukuba Central, Abe, Koji; National Institute of Advanced Industrial Science and Technology Tsukuba Center Tsukuba Central Manabe, Kengo; National Institute of Advanced Industrial Science and Technology Tsukuba Center Tsukuba Central, Research Institute for Advanced Electronics and Photonics Saito, Koichiro; National Institute of Advanced Industrial Science and Technology Tsukuba Center Tsukuba Central, Electronics and Photonics Research Institute

Photo-controllable Azobenzene Microdroplets on an Open Surface and their Application as Transporters

Yasuo Norikane, Mio Ohnuma, Dennis Kwaria,, Yoshihiro Kikkawa, Takuya Ohzono, Toshiko Mizokuro, Koji Abe, Kengo Manabe, and Koichiro Saito

New Concepts

We demonstrate a new and simple method for light-driven manipulation of microdroplet on an open-surface. Unlike conventional methods for light-based droplet manipulation, which often require tedious surface modification and complex control of light sources (including on/off switching, changing the wavelength, and single droplet tracking), our method allows continuous motion of droplets composed of photoresponsive compounds during irradiation. Furthermore, this technique enables the simultaneous control of multiple droplets, and the direction of their motion can be readily changed by changing the positions of light sources. The finding of this study opens up exciting possibilities for the development of innovative light-driven open-surface microfluidic systems.

COMMUNICATION

Photo-controllable Azobenzene Microdroplets on an Open Surface and their Application as Transporters

Yasuo Norikane,*[a,b] Mio Ohnuma,[a] Dennis Kwaria,[a] Yoshihiro Kikkawa,[a] Takuya Ohzono,[a] Toshiko Mizokuro,[a] Koji Abe,[a] Kengo Manabe,[a] and Koichiro Saito[a]

The control of droplet motion is a significant challenge, as there has been no simple method for effective manipulation. Utilizing light for the control of droplets offer a promising solution due to its non-contact nature and high degree of controllability. In this study, we present our findings on the translational motion of pre-photomelted droplets composed of azobenzene derivatives on a glass surface when exposed to UV and visible light sources from different directions. These droplets exhibited directional and continuous motion upon light irradiation and this motion was size dependent. Only droplets with diameters less than 10 μm moved with a maximum velocity of 300 μm/min. In addition, the direction of the movement was controllable by the direction of the light. The motion is driven by a change in contact angle, where UV or visible light switched the contact angle to approximately 50° or 35°, respectively. In addition, these droplets were also found to be capable carriers for fluorescent quantum dots. As such, droplets composed of photoresponsive molecules offer unique opportunities for designing novel light-driven open-surface microfluidic systems.

Introduction

The controllable manipulation of droplet motion is essential for various applications, including printing, heat transfer, clinical diagnostics, etc.[1–4] In particular, the programmable transport of droplets on solid surfaces has been attracting considerable attention because of its significance in numerous applications including microreactors,[5,6] biomedical equipment[7–9], and surface/microfluidics.[10–12] Furthermore, droplet-based microfluidic systems are becoming popular as pumps are not required, leading to an inexpensive and easy device construction.[10,13–15] The methods employed for the precise control of droplet motion are either passive or active, where droplet motions are generated in the former method without external energy stimuli,[16–20] whereas the latter requires the use of an additional energy input. Passive droplet manipulation can be achieved by creating wettability gradients on the surface[16–18] or by chemical functionalization[19,20]. However, in this method, the droplets move in one direction, and their motion cannot be changed during the process. In contrast, the active droplet strategy allows us to control the motion of droplets on demand, including the moving direction and start-and-stop control. Active techniques for droplet manipulation can be categorized based on the nature of the external energy input into electrical,[21,22] magnetic,[23–26] thermal,[27–30] and optical controls.[31–35]

Among these methods, magnetic control is a promising method for droplet transport. Previous studies have achieved droplet transportation by incorporating magnetic particles into the droplets[36] or by manipulating structures responsive to magnetic fields.[37] However, several challenges remain such as effectively separating the magnetic particles from the droplet without altering the substrate, and preventing materials from penetrating into the uneven structure. Consequently, it has become difficult to use micro-droplets and droplets as carriers. In contrast, manipulation of materials through light control represents a more versatile approach. Light-based techniques, in particular, have attracted significant attention due to their non-contact nature, controllability, and the underlying molecular-level driving mechanism.[38,39] For example, directional motion of liquid droplets has been successfully demonstrated on functionalized surfaces using photoresponsive molecules such as azobenzene[34] and rotaxane.[33] In these studies, surface gradients generated by the photoswitching molecules led to the directional motion of the droplets. Our research group has also achieved the transportation of objects on millimeter-scale droplets using a

a. Research Institute for Advanced Electronics and Photonics, National Institute of Advanced Industrial Science and Technology (AIST), Tsukuba, Ibaraki, 305-8565, Japan. E-mail: y-norikane@aist.go.jp
b. Faculty of Pure and Applied Sciences, University of Tsukuba, Ibaraki, 305-8571, Japan
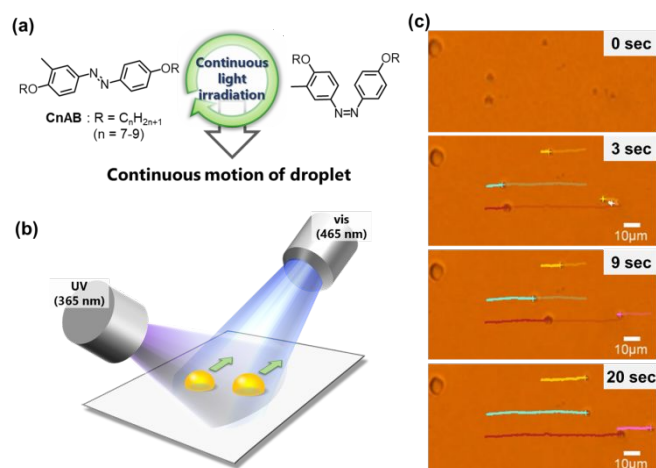
Fig. 1 (a) Structures, isomerization of CnAB derivatives, along with the concept of crawling motion under continuous light irradiation. (b) Schematic representation of the experimental setup and the motion of the droplets. (c) Photomicrographs of the crawling motion of C8AB. The colored lines represent the trace of trajectory of the droplet.

Fig. 2 (a-b) Snapshots of the crawling droplets of C8AB. Colored dashed circles highlight the specific motion. (a) A droplet chases other droplets and merges into one droplet. (b) Droplets collapse into a large crystal. (c) Travel distance of selected droplets during the motion. Numbers indicate the identification number of droplets. See Figure S1 for the numbering. (d) Dependence of droplet (or crystal) diameter on the velocity during the crawling motion observed in SI Movie 2. Scale bar: 20 μm.

photoresponsive fluid layer.[31] However, it is notable that these methods require surface functionalization and the intricate control of the light source, including timely on/off switching, changing the wavelength, and tracking the position of the moving droplet. Therefore, achieving the continuous motion and manipulating multiple droplets simultaneously has proven to be challenging.

Recently, our research group reported the continuous translational (crawling) motion of crystals composed of simple azobenzene derivatives (3,3'-dimethylazobenzene[40] and 4-(methylamino)azobenzene[41]) on a glass surface without the need for either special functionalization of the surface or for tracking by a light source. The proposed method required a simple experimental setup, where the exposure to either one or two light sources enabled the controllable motion of multiple crystals. However, this method has only been applied to move crystals which have inherent issues on the speed and difficulties into mixing with other substances to carry.

Herein, we report the continuous motion of liquid droplets of azobenzene derivatives (CnAB, Figure 1(a)) on a glass surface under continuous UV and visible light irradiation. This phenomenon was serendipitously found during our exploration of crawling crystals.[40,41] The liquid droplets reversibly deform with a change in the contact angle by light irradiation. Exposure to the two light sources induced a surface tension gradient over the droplet surface and which induced motion. The direction of the droplets was controlled by changing the position of the light. In addition, the application of these droplets as transporters to carry nanoparticles on a glass surface was also demonstrated. As far as we know, this is the first report of continuous droplet motion driven by the photoreaction of the droplet itself at a solid/air interface, along with its ability to transport small particles.

Results and discussion

Droplet motion on continuous irradiation

The compounds used in this study were CnAB derivatives bearing a methyl group at the *meta* position and two long alkyl chains (n = 6-10) linked to the *para* positions via oxygen atoms (Figure 1(a)). They were originally developed by our group as compounds exhibiting a photochemically-induced solid–liquid phase transition (photomelting) by light irradiation.[42,43] These compounds melt or crystallize upon exposure to UV or visible (blue) light, respectively. However, they do not crystallize and remain as liquid droplets even upon visible-light exposure when the particle size is small.

Upon the simultaneous exposure of the photomelted droplets on a hydrophilic glass to both UV and visible light under the experimental setup shown in Figure 1(b), translational motion was observed (Figure 1(c) and SI Movie 1). The droplets travelled approximately 50 μm in 10 s, while the moving velocity of previously reported crawling crystals[40,41] was limited to 4 μm/min. Furthermore, the motion was almost continuous upon light exposure where the droplets moved away from the UV light source toward the visible source; and thus, followed a motion trend similar to that of crystals.[40]
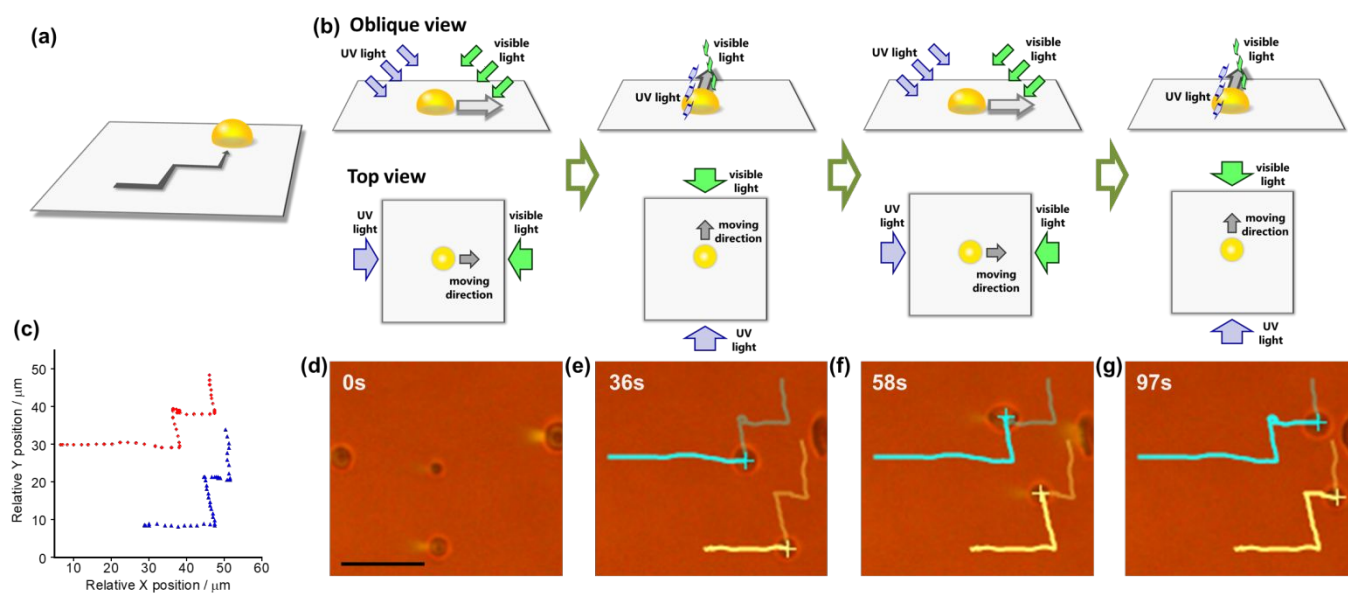
Fig. 3 (a) Schematic illustration of the zigzag motion. (b) Schematic representation of the irradiation sequence in the oblique view and in the top view. (c) Trajectory plot of the droplet during the zigzag motion. Each marker is plotted with an interval of about 1.6 seconds. (d–g) Snapshots of the zigzag motion of the droplets. Time indicates the elapsed time from the first snapshot. Colored lines indicate the trajectory of the droplet. Scale bar: 20 µm.

It should be noted that many droplets moved simultaneously across the entire field of view of the microscope (SI Movie 2). When two droplets encountered each other (Figure 2(a), SI Movie 2), they merged and continued moving. When these moving droplets collapsed into a large crystal, they were trapped in and became part of it (Figure 2(b), SI Movie 2). When the motion was not obstructed, the droplet could move continuously within the field of view of the microscope. Figure 2(c) shows the travel distance of the six selected droplets observed in the video (SI Movie 2). The speed of the droplets were in the 250–300 µm min^{-1} range; consequently these droplets were 100 times faster than the crawling crystals,[40,41] thus indicating that the present phenomena were completely different from those previously reported. Figure 2(d) shows the relationship between the size and velocity by analyzing all the droplets and crystals in the video in SI movie 2. Interestingly, only droplets with diameters less than 10 µm exhibited motion, thus indicating extreme size selectivity. To investigate the reproducibility of this trend, other samples were prepared and the same trend was observed. Although precisely determining the lower size limit was difficult due to the limited resolution of the optical microscope, the graph in Figure 2(d) indicated that droplets smaller than 3 µm could not move.

Making a zigzag motion
Changing the position of the light sources resulted in a zigzag motion (Figure 3 and SI Movie 3). Irradiating the sample with UV and visible light sources from the left and the right, respectively, resulted in the motion of the droplets to the right (Figure 3(d-e)), while changing the position of the light sources to the front and back, respectively, changed the direction by 90° and resulted in the motion to the back (Figure 3(e-f)). By repeatedly

changing the direction of the light source, the zigzag motion continued, thus indicating the ability of the light source to remotely control the motion of the droplets. Interestingly, a deformation of the droplet was observed as it moved. The
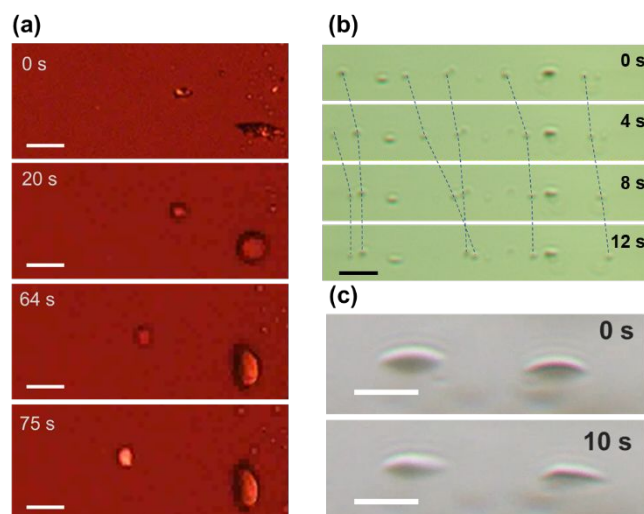
Fig. 4 (a) Snapshots of the crawling behavior of C8AB observed by a polarizing optical microscope. The angle between the analyzer and the polarizer of the POM was ca. 80° to enable a clearer observation of the isotropic liquid. (b) Snapshots of the crawling behavior of C8AB droplets observed from the side. Dashed lines indicate the same droplets. (c) Asymmetric deformation of C8AB droplets observed upon exposure to UV light (365 nm) and visible light (465 nm) lights. Time indicates the elapsed time from the initial snapshot. Scale bars: 20 µm.

droplets contracted along the direction of the motion and extended perpendicular to it (Figure 3(d-g) and SI Movie 3). This deformation of droplets was also observed in the moving droplets in SI Movie 2. This might be attributed to the change in the contact angle and will be discussed later, along with the data observed from the side of the droplet.
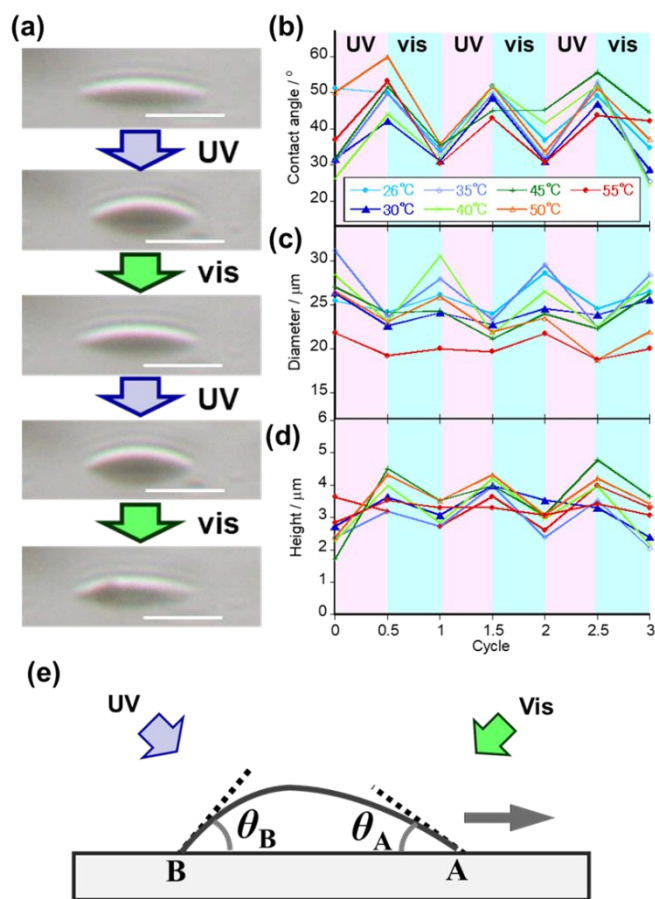
Fig. 5 Deformation of C8AB droplets upon alternating irradiation of UV light (365 nm) and visible light (465 nm). Snapshots of the deformation (a). Changes in the contact angle (b), diameter (c), and height (d) of the droplet in the 26–55°C range. Scale bar: 20 μm. (e) Schematic illustration of the asymmetric deformation and droplet motion. θ_A and θ_B represent the contact angles of the droplet at points A and B, respectively.

Shape of droplets
To further confirm that these particles were in fact droplets and not crystals, the motion was observed using a polarizing optical microscope (Figure 4(a)). Initially, C8AB showed a crystalline phase, as observed by the bright images, due to its birefringence (Figure 4(a), 0 s). Upon their irradiation by UV light, the C8AB droplets lost their birefringence and photomelted, where the image of the brightly observed particles darkened (Figure 4(a), 20 s) due to the loss of birefringence. Upon exposure to visible light, some particles started moving with the dark images being maintained (Figure

4(a), 64 s). It should be noted that these moving objects did not exhibit any birefringence. Significantly, birefringence suddenly appeared when they stopped moving (Figure 4(a), 75 s, and SI Movie 4). These results clearly indicated that the moving objects were in the liquid phase.

To gain further information on the shape of the droplet, the motion was observed from the side using an optical setup shown in Figure S5. Figure 4(b) and SI Movie 5 show the motion of the droplets upon their exposure to UV and visible lights. Interestingly, we found that the droplets had an asymmetric shape under light irradiation (Figure 4(c) and SI Movie 6). When the sample was exposed to UV and visible light to induce motion, the droplets in Figure 4(c) moved slightly before stopping. The asymmetric shape of the droplet was confirmed as the contact angle of the left side (facing UV light) of the droplet was larger than that of the right side (facing the visible light). This deformation was consistent with the observation that the droplets contracted with respect to the direction of the motion (SI Movie 3). Under the experimental conditions shown in SI Movie 6, this phenomenon was more prominent in droplets with larger sizes (> ~ 15 μm).

Alternating contact angle by light irradiation
These observations indicated the alteration of the contact angle of the droplet by photoirradiation. The droplets were then irradiated alternately with either UV or visible light using the same experimental setup, and distinct changes in the shape were observed (Figure 5(a) and SI Movie 7). The drop swelled, and the contact angle increased upon UV irradiation, while visible light irradiation flattened the droplet, and decreased the contact angle. By continuously alternating the light sources, the droplets exhibited reversible shape changes while maintaining symmetry with respect to the surface normal, which was maintained even when light was irradiated from an oblique direction. The contact angles after irradiation with UV and visible light at room temperature (26°C) were 50° and 35°, respectively. Light irradiation altered the diameter and height of the droplets as well as the contact angle (Figure 5(b)). The UV light decreased the diameter and increased in height, while in the presence of visible light, an opposite phenomenon was observed. Droplet deformation was observed over a wide temperature range (Figure 5(b)–(d)). The surface tension values of the UV and visible light-exposed droplets were 66.7 and 47.6 mN m^{-1}, respectively. These values were obtained using the Zisman plot[44] (Figure S6). The higher surface tension obtained after UV irradiation can be attributed to the higher dipole moment in the cis isomer. Surface tension is attributed to molecular interactions, and thus, the presence of the cis isomer provided more molecular interactions, which increased surface tension. Figure S10 shows that cis and trans isomers are predominantly present by 365 nm and 465 nm irradiation, respectively. Based on these results, along with those presented in Figure S6, we concluded that the contact angles are primary influenced by the isomer ratio.

The droplet deformation of C8AB described above is illustrated in Figure 5(e). The droplet had an asymmetric shape with higher and lower contact angles at the rear (UV, θ_B) and front (vis, θ_A)

COMMUNICATION
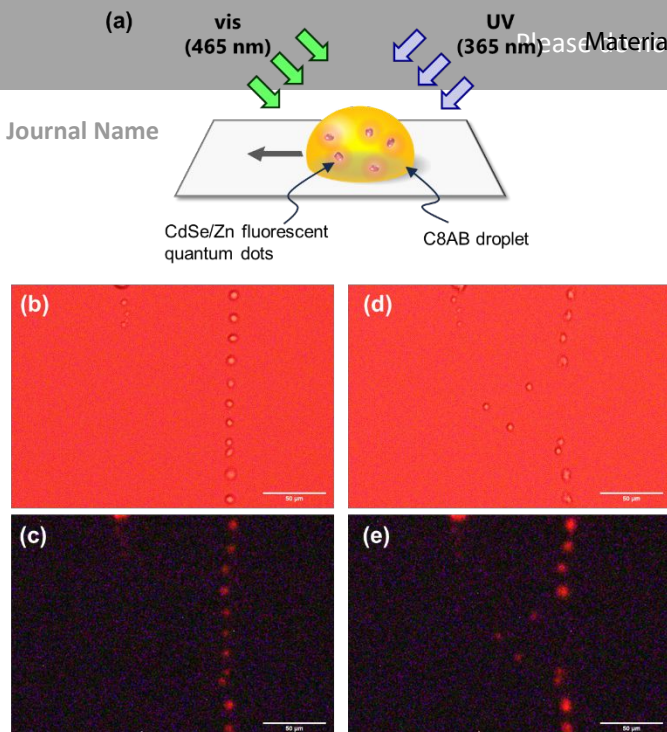
Fig. 6 (a) Schematic representation of the droplets of C8AB carrying fluorescent quantum dots. Optical ((b) and (d)) and fluorescence ((c) and (e)) microscopic images of the droplets before ((b) and (c)) and after ((d) and (e)) irradiation. The exposure time was 30 seconds. Scale bar: 50 μm.

sides, respectively. Therefore, the Laplace pressure was greater at the rear end, and the droplet moved to the right. This principle of droplet motion has been previously reported.[20,45,46] However, to the best of our knowledge, this is the first report of droplet motion driven by the photoreaction of the droplet itself at a solid/air interface. The asymmetric droplet shape was attributed to the concentration gradient of the trans/cis isomers induced by the two light sources. The light penetration depth of each wavelength varied depending on the position of the droplet, which created a gradient of the isomer ratio; this is similar to the discussion in the crystal system.[47] Regarding the observed size-selected motion, the blurring of the gradient on the smaller droplets can be attributed to the increase in the penetration depths of both light sources and the increased resistance of hydrodynamics. The larger pinning effects of the larger droplets may disturb their motions.

The net spreading tension at A and B are given by:[46]

$$t^A = \gamma_S - \gamma_{SL}^A - \gamma_L^A \cos\theta_A \quad (1)$$

$$t^B = \gamma_S - \gamma_{SL}^B - \gamma_L^B \cos\theta_B \quad (2)$$

where γ_S is the surface tension of the solid, γ_{SL}^A and γ_{SL}^B are the surface tension of solid/liquid interface at point A and B, respectively, γ_L^A and γ_L^B are the surface tension of liquid at point A and B, respectively, and θ_A and θ_B are the contact angle at point A and B, respectively. Without light exposure, the surface tension of the droplet is at an equilibrium state and it does not move, so that $t^A = t^B = 0$. Upon the exposure of two light sources, the droplet moves to the right. In this situation, we expect $t^A > 0$ and $t^B < 0$ and the contacting points A and B move to the direction where both t^A and t^B become toward zero, resulting in the motion of the droplets. Actually, continuity of the motion can be attributed to the fact that they do not become zero during motion.

In the current situation, understanding the isomer distribution at a specific position of a single droplet is quite challenging. However, when a droplet is irradiated by a single light source from an oblique direction, we believe that the isomer distribution can quickly equilibrate to a certain value due to convection inside the droplet. This equilibration should occur rapidly because of the small droplet size. Even if there is a gradient of isomer distribution, it is not sufficient to produce an asymmetric shape. On the other hand, when the droplet is irradiated by two light sources, a different isomer distribution can be established, and the distribution can be "fixed" by continuous irradiation.

Although photochemical processes are the main driving force for motion, there is still the possibility of a thermal gradient.[45,48,49] Different light sources have different intensities and absorptivities, which may create a thermal gradient. Although a temperature increase of approximately 2°C was observed, a clear temperature gradient using our IR camera could not be detected (Figure. S7), thus suggesting that the temperature gradient effect on the droplet motion may be minor.

Dependence of photoresponsive compounds and surfaces

To examine the generality of this droplet motion, azobenzene derivatives with different chain lengths were investigated. C7AB had a faster droplet motion (ca. 400 μm min⁻¹) than C8AB; however, this motion stopped as the droplets crystallized. C9AB also exhibited motion with an average velocity of ca. 250 μm min⁻¹. In this case, the droplets travelled a long distance (~ 120 μm), but a higher intensity of light was required. The photomelting of the crystals of C7AB and C9AB under the experimental conditions used was difficult, and this hindered the formation of stable and mobile droplets. The difference in the droplet speed might be attributed to the viscosity since molecules with longer alkyl chains are more viscous, which may slow down the motion. C6AB and C10AB barely moved, as the crystals did not completely melt by photoirradiation at room temperature. These results indicated that the stability of the melted droplets is a must in this molecular system. In the molecular design of CnAB, C8AB showed the best photomelting property among the n = 1–18 alkyl chain derivatives.[43]

The possibility of achieving motion on another hydrophilic surface, mica, was investigated. Although a slight fluctuation of the droplets was observed during the exposure, it was found that the C8AB droplet showed a similar motion (Figure S8). The effect of different surface properties on this motion is intriguing, and a detailed exploration of this issue in the future will contribute to revealing the mechanism of motion.

Transporting quantum dots

Recently, open-space microfluidic systems have attracted attention because of their simple fabrication and their wide application in the chemical, biomedical, and environmental fields.[50–52] To control the mobility, various studies have demonstrated stimuli-responsive liquids in open fluidic settings, but these methods require complicated surface preparation and tedious light tracking.[10,53] Here, the ability of the

azobenzene droplet to carry fluorescent probes was investigated as shown in Figure 6(a). Generally, azobenzenes do not emit fluorescence because of their low quantum yields, which compete with fast nonradiative processes such as isomerization and internal conversion.[54] In fact, the light source does not only result in the crawling motion, but it can also excite appropriate fluorescent probes. Consequently, it is possible to simultaneously observe fluorescence upon the motion of the droplets. CdSe/ZnS core-shell type was selected as the quantum dot owing to its high fluorescence quantum yield (≥ 0.50) and emission wavelength (655–675 nm). A mixture of C8AB and the quantum dots placed on a glass substrate was exposed to two light sources under conditions similar to those used in the above experiments and red emission was observed, which was attributed to the quantum dots in the C8AB droplets. Furthermore, the red-emitting droplets moved upon light irradiation, (Figure 6(b-e) and SI Movie 8), thus indicating that the quantum dots were carried by the C8AB. The travelling distance of the droplets during an exposure time of 140 s was plotted. Notably, the size selectivity trend was similar to that of the droplets without the quantum dots (Figure S9).

Conclusions

In summary, we have successfully achieved continuous motion and simultaneous manipulation of multiple droplets. This was accomplished by utilizing controllable microdroplets of photoresponsive molecules on a hydrophilic glass through simultaneous irradiation with UV light (365 nm) and visible light (465 nm) from opposite directions. The key findings of this study include continuous motion throughout the irradiation, reaching speeds of approximately 300 μm min^{-1}, a significant improvement over crawling crystals.[40,41] The direction of the motion was determined by the positions of the light sources, with the droplets moving away from the UV light. Changing the light source position allowed for altering the direction of the droplets. Importantly, droplets with sizes less than 10 μm exhibited this unique motion, highlighting its size-dependent nature. Furthermore, we observed reversible changes in the contact angle and shape of the droplets upon alternating irradiation at 365 and 465 nm. This reversible alteration in surface tension led to asymmetric deformation and droplet motion. These photo-controllable droplets also served as micrometer-sized carriers for transporting fluorescent quantum dots. The insights gained in this study will contribute to the development of a method to manipulate droplets on a dry, open surface without the need for gradient fabrication.

Author Contributions

M.O. conducted the experiments; D.K. helped with the synthesis of compounds; Y.K. helped with the preparation of surfaces; T.M. and K.S. helped with the transportation experiments; T.O., K.A., and K.M. helped with the analysis and discussion of the data; Y.N. initiated and guided the work and drafted the manuscript. All authors contributed to the discussion and preparation of the manuscript. All authors have given approval to the final version of the manuscript.

Conflicts of interest

There are no conflicts to declare.

Acknowledgements

Notes and references

1   Y. Zuo, L. Zheng, C. Zhao and H. Liu, *Small*, 2020, **16**, 1903849.
2   R. Malinowski, I. P. Parkin and G. Volpe, *Chem. Soc. Rev.*, 2020, **49**, 7879–7892.
3   H. Liu, L. Zhang, J. Huang, J. Mao, Z. Chen, Q. Mao, M. Ge and Y. Lai, *Adv. Colloid Interface Sci.*, 2022, **300**, 102584.
4   S. Liu, L. Lin and H. B. Sun, *ACS Nano*, 2021, **15**, 5925–5943.
5   W. H. Tan and S. Takeuchi, *Lab Chip*, 2006, **6**, 757–763.
6   L. Frenz, A. El Harrak, M. Pauly, S. Bégin-Colin, A. D. Griffiths and J. C. Baret, *Angew. Chemie - Int. Ed.*, 2008, **47**, 6817–6820.
7   G. Huang, M. Li, Q. Yang, Y. Li, H. Liu, H. Yang and F. Xu, *ACS Appl. Mater. Interfaces*, 2017, **9**, 1155–1166.
8   C. J. Huang, W. F. Fang, M. S. Ke, H. Y. E. Chou and J. T. Yang, *Lab Chip*, 2014, **14**, 2057–2062.
9   Y. Zhang, S. Park, K. Liu, J. Tsuan, S. Yang and T. H. Wang, *Lab Chip*, 2011, **11**, 398–406.
10   Y. Xu, A. M. Rather, Y. Yao, J. Fang, R. S. Mamtani, R. K. A. Bennett, R. G. Atta, S. Adera, U. Tkalec and X. Wang, *Sci. Adv.*, 2021, **7**, eabi7607.
11   G. V. Kaigala, R. D. Lovchik and E. Delamarche, *Angew. Chemie - Int. Ed.*, 2012, **51**, 11224–11240.
12   R. Seemann, M. Brinkmann, T. Pfohl and S. Herminghaus, *Reports Prog. Phys.*, 2012, **75**, 016601.
13   M. Elsharkawy, T. M. Schutzius and C. M. Megaridis, *Lab Chip*, 2014, **14**, 1168–1175.
14   M. M. Thuo, R. V. Martinez, W. J. Lan, X. Liu, J. Barber, M. B. J. Atkinson, D. Bandarage, J. F. Bloch and G. M. Whitesides, *Chem. Mater.*, 2014, **26**, 4230–4237.
15   C. Li, M. Boban, S. A. Snyder, S. P. R. Kobaku, G. Kwon, G. Mehta and A. Tuteja, *Adv. Funct. Mater.*, 2016, **26**, 6121–6131.
16   Z. Zhang, F. Zhang, Q. Huang, G. Cheng and J. Ding, *Appl. Surf. Sci.*, 2020, **515**, 145976.
17   N. A. Malvadkar, M. J. Hancock, K. Sekeroglu, W. J. Dressick and M. C. Demirel, *Nat. Mater.*, 2010, **9**, 1023–1028.
18   A. Shastry, M. J. Case and K. F. Böhringer, *Langmuir*, 2006, **22**, 6161–6167.
19   S. Daniel, M. K. Chaudhury and J. C. Chen, *Science*, 2001, **291**, 633–636.

20   M. K. Chaudhury and G. M. Whitesides, *Science*, 1992, **256**, 1539–1541.
21   J. Li, N. S. Ha, T. 'Leo' Liu, R. M. van Dam and C.-J. 'CJ' Kim, *Nature*, 2019, **572**, 507–510.
22   A. R. Wheeler, *Science*, 2008, **322**, 539–540.
23   X. Liu, N. Kent, A. Ceballos, R. Streubel, Y. Jiang, Y. Chai, P. Y. Kim, J. Forth, F. Hellman, S. Shi, D. Wang, B. A. Helms and P. D. Ashby, *Science*, 2019, **365**, 264–267.
24   W. Wang, J. V. I. Timonen, A. Carlson, D. M. Drotlef, C. T. Zhang, S. Kolle, A. Grinthal, T. S. Wong, B. Hatton, S. H. Kang, S. Kennedy, J. Chi, R. T. Blough, M. Sitti, L. Mahadevan and J. Aizenberg, *Nature*, 2018, **559**, 77–82.
25   H. Lin, W. Yu, K. A. Sabet, M. Bogumil, Y. Zhao, J. Hambalek, S. Lin, S. Chandrasekaran, O. Garner, D. Di Carlo and S. Emaminejad, *Nature*, 2022, **611**, 570–577.
26   Z. Sheng, M. Zhang, J. Liu, P. Malgaretti, J. Li, S. Wang, W. Lv, R. Zhang, Y. Fan, Y. Zhang, X. Chen and X. Hou, *Natl. Sci. Rev.*, 2021, **8**, nwaa301.
27   A. Bouillant, T. Mouterde, P. Bourrianne, A. Lagarde, C. Clanet and D. Quéré, *Nat. Phys.*, 2018, **14**, 1188–1192.
28   N. J. Cira, A. Benusiglio and M. Prakash, *Nature*, 2015, **519**, 446–450.
29   H. Hwang, P. Papadopoulos, S. Fujii and S. Wooh, *Adv. Funct. Mater.*, 2022, **32**, 1–9.
30   Y. Shen, Y. Yuan, T. Tang, N. Ota, N. Tanaka, Y. Hosokawa, Y. Yalikun and Y. Tanaka, *Sensors Actuators B Chem.*, 2022, **358**, 131511.
31   K. Manabe, K. Saito, M. Nakano, T. Ohzono and Y. Norikane, *ACS Nano*, 2022, **16**, 16353–16362.
32   J. Lv, Y. Liu, J. Wei, E. Chen, L. Qin and Y. Yu, *Nature*, 2016, **537**, 179–184.
33   J. Berna, D. Leigh, M. Lubomska, S. Mendoza, E. Perez, P. Rudolf, G. Teobaldi and F. Zerbetto, *Nat. Mater.*, 2005, **4**, 704–710.
34   K. Ichimura, S.-K. Oh and M. Nakagawa, *Science*, 2000, **288**, 1624–1626.
35   J. Zheng, J. Chen, Y. Jin, Y. Wen, Y. Mu, C. Wu, Y. Wang, P. Tong, Z. Li, X. Hou and J. Tang, *Nature*, 2023, **617**, 499–506.
36   A. Li, H. Li, Z. Li, Z. Zhao, K. Li, M. Li and Y. Song, *Sci. Adv.*, 2020, **6**, 1–7.
37   S. Jiang, Y. Hu, H. Wu, R. Li, Y. Zhang, C. Chen, C. Xue, B. Xu, W. Zhu, J. Li, D. Wu and J. Chu, *Nano Lett.*, 2020, **20**, 7519–7529.
38   D. Baigl, *Lab Chip*, 2012, **12**, 3637–3653.
39   A. Goulet-Hanssens, F. Eisenreich and S. Hecht, *Adv. Mater.*, 2020, **32**, 1905966.
40   E. Uchida, R. Azumi and Y. Norikane, *Nat. Commun.*, 2015, **6**, 7310.
41   K. Saito, M. Ohnuma and Y. Norikane, *Chem. Commun.*, 2019, **55**, 9303–9306.
42   Y. Norikane, E. Uchida, S. Tanaka, K. Fujiwara, E. Koyama, R. Azumi, H. Akiyama, H. Kihara and M. Yoshida, *Org. Lett.*, 2014, **16**, 5012–5015.
43   Y. Norikane, E. Uchida, S. Tanaka, K. Fujiwara, H. Nagai and H. Akiyama, *J. Photopolym. Sci. Technol.*, 2016, **29**, 149–157.
44   W. A. Zisman, in *Contact Angle, Wettability, and Adhesion in Advances in Chemistry Series*, ed. F. M. Fowkes, American Chemical Society, 1964, vol. 43, pp. 1–51.
45   P.-G. de Gennes, F. B. Brochard-Wyart and D. Quere, *Capillarity and Wetting Phenomena Drops, Bubbles, Pearls, Waves*, Springer, New York, 2004.
46   S. K. Oh, M. Nakagawa and K. Ichimura, *J. Mater. Chem.*, 2002, **12**, 2262–2269.
47   Y. Norikane, M. Hayashino, M. Ohnuma, K. Abe, Y. Kikkawa, K. Saito, K. Manabe, K. Miyake, M. Nakano and N. Takada, *Front. Chem.*, 2021, **9**, 684767.
48   F. Brochard, *Langmuir*, 1989, **5**, 432–438.
49   J. B. Brzoska, F. Brochard-Wyart and F. Rondelez, *Langmuir*, 1993, **9**, 2220–2224.
50   J. Berthier, K. A. Brakke and E. Berthier, *Open Microfluidics*, Scrivener Publishing, Beverly, MA, 2016.
51   S. T. Wu, C. Y. Huang, C. C. Weng, C. C. Chang, B. R. Li and C. S. Hsu, *ACS Omega*, 2019, **4**, 16292–16299.
52   Y. Xu, Y. Chang, Y. Yao, M. Zhang, R. L. Dupont, A. M. Rather, X. Bao and X. Wang, *Adv. Mater.*, 2022, **34**, 1–11.
53   W. Li, X. Tang and L. Wang, *Sci. Adv.*, 2020, **6**, eabc1693.
54   H. M. D. Bandara and S. C. Burdette, *Chem. Soc. Rev.*, 2012, **41**, 1809–1825.